University of Nevada, Reno

Applications in Traffic Analysis from Automatically Extracted Road User Interactions with Roadside LiDAR Trajectories

A thesis submitted in partial fulfillment of the

requirements for the Master of Science in

Civil Engineering

by

Trevor Whitley

Dr. Hao Xu/Thesis Advisor

May 2022

THE GRADUATE SCHOOL

We recommend that the thesis
prepared under our supervision by

entitled

be accepted in partial fulfillment of the
requirements for the degree of

Advisor

Committee Member

Committee Member

Graduate School Representative

David W. Zeh, Ph.D., Dean
Graduate School

Abstract

Traffic trajectory data extracted from sensors such as LiDAR and camera has birthed new research areas in the field of transportation. Traffic trajectories is defined at the ability to track road users through time and space at high frequency, typically every tenth of a second. Given this higher granularity of micro traffic data, the behavior of road users can be explored to understand the operational and safety performances on the roads. Therefore, researchers have been stretching the limits to what this type of data can be applied to. Most studies look into the interactions of road users as a surrogate safety measure (SSM) to identify potentially dangerous situation using measures such as post encroachment time (PET) or time to collision (TTC); however, not much applications have been explored outside this. This paper seeks to stretch the imagination for what this type of data can be used for using trajectories generated from roadside LiDAR cloud point data. The first application presented in this paper introduces the first automated method to extract headways and determine capacities at roundabouts entry legs. The method provided accurate capacity results when compared to other standard methods. The second application proposes an automated method to extract pedestrian-vehicle yield rates at uncontrolled crosswalks Pedestrian-vehicle interaction (PVI) analyses from trajectory data has been studied using the SSMs mentioned, but an analysis on yield rates using trajectory data has seldom been performed. This research in traffic trajectory applications paves the way for further applications in traffic safety, operations, and planning.

Table of Contents

List of Tables

List of Figures

Introduction

The introduction section will outline general concepts for both roundabout capacity analysis and pedestrian-vehicle interactions and introduce the methodologies presented in this paper and their implications on the transportation profession.

Roundabout Capacity

Roundabouts are circular intersections where the entry is yield controlled and the circulatory lane(s) is an uninterrupted flow circulating a central island (counterclockwise in the United States) (TRB 2016). Operational performance at roundabouts has been a big topic since the emergence of roundabouts in the United States in the 1990s and since then, their popularity has grown (Ahiamadi *et al.* 2012). Roundabouts are generally known to reduce delay for low to medium traffic volumes and are also regarded as safer alternatives because of reduction in conflict zones, elimination of head-on and angle crashes, reduction in speed, and reduction of vehicular delay and stops (Ahiamadi *et al.* 2012). As a result of improved operational performance, roundabouts are known to produce lower emissions when compared to other intersection controls at low to medium traffic volumes (Ahiamadi *et al.* 2012).

"Capacity represents the maximum sustainable hourly flow rate at which persons or vehicles reasonably can be expected to traverse a point or a uniform segment of a lane or roadway during a given time period under prevailing roadway, environmental, traffic, and control conditions" (TRB 2016). There have been many proposed methods for computing capacity at roundabouts either by regression models or analytic models, but the industry of traffic engineering utilizes the Highway Capacity Manual as a guide to measuring capacity and other performance measures such as level of service (LOS), delay, queue, and volume-to-capacity ratio. For roundabouts, HCM employs a combination of regression and analytic models to derive a relationship between conflicting traffic flow and capacity of entry flow. For roundabouts, the conflicting traffic flow is the circulating flow, and the capacity of the entry is at the entry lanes of the roundabout leg. The entry capacity decreases as the conflicting circular flow increases. The analytic model that the HCM employs is based on the gap acceptance theory.

Gap acceptance theory has been a useful model to explain the two-way stopped controlled intersections where a minor stream vehicle needs to decide which gap or headway is large enough to enter into the major stream traffic. For the case of roundabouts, the minor stream refers to the entry lane(s) which is yield controlled and the major stream refers to the circulatory lane(s). The minor stream driver is referred to as the decision vehicle. The headway with which the decision driver is willing to 'accept' and enter the major stream flow is a function of many factors such as the driver's experience, environmental factors, geometric design, speed, traffic volume, and more. The tendency for the decision driver to either reject or accept a headway is captured by measuring the critical headway. The critical headway is the minimum time headway between two successive major stream vehicles for which the minor stream decision vehicle can make a maneuver to enter the major stream (Ahiamadi *et al.* 2012). Critical headway is one of the gap acceptance parameters used. The second gap acceptance parameter is follow-up headway, which is the time headway between the departure of one minor stream vehicle and the departure of the subsequent minor stream vehicle into the major stream utilizing the same gap under the condition of continuous queueing (Ahiamadi *et al.* 2012). The HCM determines these gap acceptance parameters based on field data across the United States to derive a capacity equation that is a function of the conflicting flow.

Critical headway cannot be measured directly because each driver is different, and the individual critical headway will vary from driver to driver. Further analysis of rejected headway and accepted headway from field data must be conducted. A rejected headway is the major stream headway between two successive vehicles for which a minor stream decision vehicle decides not to enter the major steam. Conversely, an accepted headway is a major stream headway between two successive vehicles for which a minor stream decision vehicle decides to enter the major stream. Therefore, many data points of rejected and accepted headways need to be collected, and further analysis is conducted to extract the critical headway. Many methods have been developed to determine the critical headway such as Raff's Method, Maximum Likelihood Method, Probability Equilibrium Method, Median Method, and many more. The Raff's Method and Maximum Likelihood Method are the two most common based on the literature. In this study, Raff's Method is employed due to its' ease of computation. The second gap acceptance parameter is

the follow-up headway, which is calculated by taking the average of the field measured follow-up headways.

Once the two gap acceptance parameters are determined, they can be used to calibrate the HCM 2016 capacity equation. As a result of observed variability between states and cities in gap acceptance parameter results, HCM has provided a method for calibrating the capacity equation for more accurate measurement of capacity at certain states, cities, and even specific roundabouts and roundabout legs. For example, Nevada has their own capacity equation developed by Ahiamadi *et al*.

Pedestrian-Vehicle Interactions

As of 2018, road traffic injuries are the leading cause of fatalities for people aged 5-29 years, according the World Health Organization (WHO). Such fatalities are disproportionately shared by vulnerable road users such pedestrians, cyclists, and motorcyclists, with nearly 20% of fatal crashes being pedestrian-related according to the 2019 FARS data. The vulnerability of a road user is measured by the relative protection, speed, and weight of the road user when compared to a vehicle (Amado et al. 2020). Despite all the proven countermeasures and capital improvements made to reduce such crashes, the issue is still prevalent. In traditional traffic safety analysis, crash data is used to identify countermeasures to reduce crashes; however, there are limitations to simply looking at crash data. Therefore, behavioral measures of road user interactions such as surrogate safety measures (SSM) can identify localized safety concerns and provide countermeasure selection in a more proactive manner.

Trajectory data extracted from sensors such as LiDAR and camera has birthed a new research area for SSM since it can track road users through time and space at a high frequency. Trajectory data can be used to measure SSM such as time to collision (TTC), post-encroachment time (PET), and deceleration rate to avoid collision (DRAC). TTC is the time to collision when two road users continue their trajectory at the same angle and speed without any kind of evasive behavior (Kizawi and Borsos, 2021). PET is the difference between times when one road user enters a conflict point until another road user arrives to the same conflict point (Kizawi and Borsos, 2021). The lower TTC and PET is, the closer to a collision the two

road users were (Kizawi and Borsos, 2021). DRAC is a measure of the vehicle's own movement which is hard deceleration rates that the vehicle must perform to avoid a collision (Jiang et al. 2021).

This paper focuses on pedestrian-vehicle interactions (PVI). In general, a PVI is defined as the moment in which the movement (trajectory) of a pedestrian and a vehicle interact or intersect, creating a conflict between road users. Perhaps the most problematic instance of PVIs is at uncontrolled crosswalks. Uncontrolled crosswalks are crossing events for which the vehicular movement is uncontrolled, but is expected to yield for any conflicting pedestrians showing intent to cross at the crosswalk. Such uncontrolled crosswalks occur at mid-block locations, roundabouts, and two- or one way stop-controlled interactions where the main street vehicle traffic conflicts with main street pedestrian crossing events.

In the case of uncontrolled crosswalks, PVIs can be defined by when a pedestrian has to slow down or stop at the curb because a vehicle is approaching, or when a vehicle decelerates, stops, or accelerated because of a pedestrian's intent to cross or during crossing. Two behaviors can be studied in such events, the behavior of the pedestrian, and the behavior of the vehicle. The most common measure of pedestrian behavior at uncontrolled crosswalks is gap time (Amado et al. 2020). In this context, the gap time is the vehicle time headway that a pedestrian is willing to cross within. In other words, gap time is a measure of the assertiveness and comfort level of the pedestrian when navigating the crosswalk; however, it can also be used to measure the risk to the pedestrian. Gap acceptance theory is a common method to measure gap time, which looks at both gaps that pedestrians accept and reject and derives a critical gap for which most of the pedestrians are willing to accept.

However, this paper focuses on the behavior of the vehicle at uncontrolled crosswalks, which is commonly measured in yield rate. The yield rate is defined as the proportion of vehicles that yield to pedestrians over all PVIs (Fu et al. 2018). This can be more accurately measured in yield compliance, which is the proportion of vehicles that yield to pedestrians over the vehicles that are physically able to yield to crossing pedestrians (Fu et al. 2018). Yield compliance essentially considers the stopping sight distance (SSD) of the vehicle, which is the perception, reaction, and braking distance most drivers are expected to stop within for a given speed. Yield rate and yield compliance can be used interchangeably, but

yield compliance is the focus of this paper. In the current literature, yield rates from PVIs are commonly extracted manually in the field or through video for the purposes of modeling and microsimulations. Therefore, high accuracy movement (trajectory) data is not considered, which captures behavior-level information at high granularity. Furthermore, there are no previous methods for automating such yield analyses leading to extensive labor hours for data extraction.

The purpose of this paper is to propose automatic methods for analyzing traffic behaviors. The first method is to automatically extract headway information for roundabouts for the purposes of determining the capacity. The second method is to automatically extract PVIs to determine yield rate at uncontrolled crosswalks. Previous studies have yet to develop such automatic methods, especially from high-resolution traffic trajectory data. Many use the method of manual extraction in the field or via video, or software to assist in generating the desired information. The implications of these methodologies are that analyses can be completed automatically upon completion of data collection which allows for faster turnover times for analysis on operational and safety performances. Further, using the high-resolution traffic trajectories, altogether more detailed analysis at the behavior level of the road user can be provided to gain greater insight on the operational and safety performances on the roads. Both methodologies employ roadside LiDAR sensors for the purposes of collecting traffic data and generating trajectory data.

The benefits that LiDAR has over video is that LiDAR is much less computationally demanding, its' 360-degree detection range makes it easier to outfit at an intersection as opposed to placing several cameras, and LiDAR is not limited by lighting condition. Therefore, LiDAR sensors can sense a wider detection range for greater periods (Zhao *et al.* 2019). Where video sensing provides high-resolution imaging, LiDAR provides high accuracy cloud points that can be used to track trajectories of all road-users such as volume, location, speed, direction, headways, and even road user size (Zhao *et al.* 2019).

The paper follows the order of literature review, methodology, case studies, conclusion, and references. The literature review covers the literature on roundabout capacity measures, PVIs, and other applications with sensor-based trajectories. The methodology section covers the data pre-processing of roadside LiDAR, the methodologies for capacity calculations at roundabouts, and the methodologies for

pedestrian-vehicle yield rate extraction. Then, the two case studies for each methodology is outlined and the results for applying the methodologies are shown. Finally, the conclusion section discusses the main finding from the study and what extended studies can be performed based on the proposed methodologies.

Literature Review

The literature review covers the literature on roundabout capacity measures, PVIs, and other applications with sensor-based trajectories.

Roundabout Capacity

A literature review of operational analysis at roundabouts is outlined. However, before jumping into the literature review, it is important to understand the key terminology such as lag, gap, and headway. The terms are defined as follows:

- Headway: the time difference between two following vehicles measured from the front bumper of the leading vehicle to the front bumper of the following vehicle.
- Gap: the time difference between two following vehicles measured from the back bumper of the leading vehicle to the front bumper of the following vehicle.
- Lag: the time difference between an entering vehicle arriving at the yield line and the next circulating vehicle arriving at the conflict zone between the two vehicles.

Since the derivation of the gap acceptance theory, there has been some confusion as to what should be measured for the critical gap, the headway or gap. The definition that has been adopted in the HCM in recent editions has been the critical headway; therefore, that is the terminology that will be used and what will be measured. However, critical gap and critical headway are used interchangeably in the literature.

In the NCHRP Report 672, "Roundabouts: An Informational Guide Second Edition", a study was conducted in 2010 as a guide for implementing roundabouts in the United States (TRB 2010). For the operational analysis section, the report mimics much of what is outlined in the HCM 2010. This informational guide defines various techniques for collecting data such as

- "Live recording of turning-movement patterns using field observers" (TRB 2010).
- "Video recording of the entire intersection followed by manual extraction of turning movement from the video" (TRB 2010).
- "Field observers at each of the exits, manually recording vehicles approaching exits" (TRB 2010).

- "Link counters at each entry, exit, and circulatory roadway in front of each splitter island, plus manual counts of right-turn movements" (TRB 2010).
- "Origin-designation survey techniques" (TRB 2010).

While these methods for data collection are well-suited for general operational performance measures, they do not help in understanding the data collection methods for extracting headway information.

In 2004, "NCHRP 3-65: Applying Roundabouts in the United States" sought to develop methods for understanding the safety and operational performance and impacts of U.S. roundabouts and refine the design criteria for implementing them (Rodergerdts 2004). This study collected data at U.S. roundabouts so domestic, rather than foreign, data can be applied for U.S. roundabouts. The data collection method that was performed in this study included a digital camcorder for providing views of entry and exits and an omnidirectional camcorder used for the operations of the entire roundabout (Rodergerdts 2004). This data collection technique allowed for the extraction of rejected lag, rejected gap, and accepted gap information (Rodergerdts 2004).

The extensive data collection in the NCHRP Report 572 and NCHRP Report 3-65 was used for developing the roundabout section of the Highway Capacity Manual 2010 (TRB 2010, USDOT 2015, Rodergerdts *et al.* 2007). As previously mentioned, the HCM has derived capacity equations to compute the entry capacity as a function of the conflicting flow rate for each lane configuration up to two lanes. The equation is derived by the gap acceptance parameters of critical headway and follow-up headway. However, the newer sixth edition of the HCM published in 2016 derives new capacity equations based on further data collection efforts. One thing to note about the difference between these two sets of capacity equations is that the HCM 2016 yields higher capacity results than the HCM 2010 (TRB 2016). The HCM 2016 addresses this by stating that "the capacity presented here are believed to be higher primarily due to the larger and more saturated dataset and not primarily due to an increase in capacity overtime" (TRB 2016). They also address the assumption that "roundabout capacity values in the United States will increase as drivers become more experienced with roundabouts", but states that "it has not been possible to provide direct evidence of this characteristic in the available data" (TRB 2016). However, the method for calibrating the capacity equation has not been changed.

In December 2012, the Center for Advanced Transportation Education and Research (CATER) at the University of Nevada, Reno (UNR) prepared the "Nevada Roundabout Implementation Guidelines" for the Nevada Department of Transportation (NDOT) where they collected data at various roundabouts in Nevada to calibrate the HCM capacity equation (Ahiamadi *et al.* 2012). This study collected data using two cameras, one to record conflicts at the entry and the other to record the traffic movements for the entire intersection (Ahiamadi *et al.* 2012). The key timestamps used for extracting the gap acceptance parameters included the enter queue time, first in queue time, exit queue time, and passage time of circulating vehicles (Ahiamadi *et al.* 2012). The Traffic Data Input Program (TPID) developed by the University of Idaho was used to assist in manually recording the key timestamps and a Microsoft Excel Macros program was used to extract the accepted headways, maximum rejected headways, and follow-up headways (Ahiamadi *et al.* 2012). Then, the maximum likelihood method was used for calculating the critical headway and an upper threshold of 8-seconds was used for the accepted headways. These same methods were applied by one of the authors of this report, Zong Z. Tian, and Feng Xu for California roundabouts, and the resulting data was used in the California capacity equation calibration for the California Department of Transportation (Xu, F., and Z. Tian 2018).

In the research paper published in 2019, Azhari *et al.* sought to estimate the critical gap at small roundabouts. They used two camcorders to capture the entry and circulatory traffic queue using the stop line as a reference and measuring the conflicting gap (headway) and lag information. This paper used 13-seconds as the upper threshold for accepted headways and used Raff's method, Wu's method, and a simple logit method (Azhari *et al.* 2019). In his paper titled "Estimating Critical Gap of Roundabouts by Different Methods", Rui-jun Guo utilized Raff's method, Ashworth's method, and the maximum likelihood method to calculate the critical headway. Guo collected video data for 40 minutes and gathered 100 maximum rejected gaps and accepted gaps (Guo 2010). In the paper "Investigation of Gap Acceptance at Roundabouts in Qatar", Hassan Ahmed Hamad provided an in-depth study of critical headway for varying lane configuration and vehicle types at various intersections in Qatar using Raff's method. Data collection was done by video and software was used to analyze the traffic conditions frame-by-frame to an accuracy of $1/30^{th}$ of a second (Hamad 2017). Hamad set a criterion for entering vehicles to come to a full stop to

observe gaps in the conflicting flow and make the decision to enter (Hamad 2017). Further studies by Hamad were conducted in the paper titled “Critical Gap between One-, Two-, and Three-Lane Roundabouts in Qatar”, which utilized the same methodology (Shaaban and Hamad 2020).

Pedestrian-Vehicle Interactions and Yield Rates

The literature review on yield rates is discussed. Yield rate is a measure of analyzing PVIs at uncontrolled pedestrian crossings, particularly driver behavior. Yielding is a critical component to measuring accessibility of and safety for pedestrians and striving to improve such measures will make streets more equitable. Most studies collect the yield data through field observations, video recordings and manual extraction, or a combination of the two (Sun et al., Ottomanelli et al., Chen et al., Lu et al., Feliciani et al.). In addition to video recordings, Schroeder et al. used a laser speed gun to collect vehicle speeds and used the data to determine when PVIs occurred. Some studies use driver simulations to measure PVIs for a variety of pedestrian crossing scenarios. The major limitations to manual field data collection methods are that it can limit the data collection time periods to day time periods. Most studies collected data during peak hours (Sun et al., Chen et al., Lu et al., Schroeder et al.). Ottomanelli et al. sought to collect data during non-peak hours to model regular conditions. Fitzpatrick and Park collected 48 hours of video recordings during daytime and nighttime periods to compare the difference in yield rates for crosswalks equipped with flashing pedestrian signals. However, to reduce the amount of manual extraction, staged pedestrians were used. A staged pedestrians is a volunteer who acts as a pedestrian and crosses at crosswalks to simulate real world PVIs. Most other studies used real PVIs without the use of staged pedestrians.

Some studies use the field collected data to develop simulation models. Lu et al. developed a cellular automata simulation model for PVI behaviors, such as vehicle yielding and pedestrian crossing behavior, at unsignalized mid-block crosswalks. Others develop statistical models with the purpose of integration into microsimulation models. Schroeder and Rouphail used a logit model to explain driver yielding behavior from data collected at two unsignalized mid-block crosswalks considering variables that can be easily implemented into microsimulations models. Logit models were among the most common models used for determining the probability of vehicle yielding to pedestrians (Sun et al., Chen et al., Lu et

al.). Another common method used is the logistic regression model, which is closely related to the logit model (Schroeder et al., Schneider et al., Fricker and Zhang).

There are many variables that can play into whether a vehicle will or will not yield for a pedestrian. Schroeder et al. showed that vehicles were more likely to yield for assertive pedestrians. Furthermore, high speeds lead to lower yield rates. Sun et al. found that opposing traffic volume, number of pedestrians waiting, and vehicle type had the greatest impact on the yielding behavior. Lu et al. also found that pedestrian groups was a significant factor in yielding behavior, but also that pedestrian attitude, vehicle time headway, and vehicle speed also contributed to the yield behavior. Schneider et al. found that vehicles were more likely to yield to white pedestrians than pedestrians of other racial or ethnic backgrounds. Fitzpatrick and Park and Coughenour et al. observed the same racial bias from their staged pedestrian studies. Schneider et al. also found that pedestrians that clearly communicating crossing intent were more likely to have drivers yield. This study also found that crosswalk locations with higher traffic and vehicle speeds were likely to have lower yield rates. Salamati et al. studied the yield behavior at roundabouts and found that yield rates were higher at the entry of the roundabout than the exit. Furthermore, Salamati et al. found the same correlation of yield behavior to vehicle speed and pedestrian groups at roundabouts. Also, it was found that yield rates at the far lane from the curb had lower yield rates than the closer lane. Bella and Nobili found that yield rates were lower for illegal crossings (jay-walkers) than legal crossings. Coughenour et al. used the estimated car cost as a predictor and found that the odds of yielding decreased 3% per $1000 increase. Infrastructure also plays a role in yield rates. Fitzpatrick and Park's study provides support for the use of pedestrian hybrid beacons (PHB), showing high daytime and nighttime yield rates. This study also showed that rectangular rapid flashing beacons (RRFB) had greater improvements for nighttime yield rates when compared to daytime.

Applications of Sensor-Based Trajectory

The literature on traffic trajectories is outlined which focuses on the application in transportation. Traffic trajectories is defined as the ability to track road users through time and space at high frequency. Essentially, the technology aims at tracking the movement of road users instantaneously. With the growing

research area in autonomous vehicles, such data has been a big research topic, with new methodologies seeking to improve the tracking accuracy of surrounding vehicles. There are two kinds of trajectory data, those obtained through GPS from connected vehicles or smart phones, and those obtained through sensor technologies. GPS connected vehicle and smart phone trajectories are collected by car or phone companies and sold to technology companies to commercialize the data for use in transportation engineering and planning. Such data typically is lower in frequency (1-3 seconds) and represents only a sample of road users. Nevertheless, it has proven to be beneficial in determining travel time, origin-destination, possible incident identification, and more. The other type of trajectory data is from sensing technologies such as camera or LiDAR. These sensors can be deployed in vehicles for autonomous driving applications, in unmanned aerial vehicle (UAV) (drones), or stationary on the roadside. Sensor-based trajectories not used for autonomous vehicle applications are generally used for more microscopic and localized traffic analyses. The frequency can be as low as one-tenth of a second or lower, with a penetration rate of theoretically 100% of road users within the detection range barring any occlusion issues. This study employs sensor-based roadside sensor trajectories, so that will be the focus of this literature review.

Cameras are most commonly used to generate trajectory data; however, the use of LiDAR sensors have become increasingly more common. Both sensors deal with the same issues of detecting, tracking, and classifying road users while also combating issues of occlusion of road users by vehicle, buildings, and other objects. Much of the applications surrounding roadside trajectory data is in behavioral analyses and surrogate safety measures (SSM) given the high frequency of road user detection. Fu et al. used vision-based trajectories from two cameras to extract PVIs and yield rates/compliance. Fu et al. used similar methods to investigate secondary PVIs at unsignalized intersection (Fu et al. 2019). Secondary PVIs are interactions between vehicles exiting the intersection and conflicting with crossing pedestrians, which are shown in the study to be more severe (Fu et al. 2019). Muppa et al. also analyzed PVIs at unsignalized interactions with vision-based trajectories, but used the surrogate safety measure of TTC to see if there is a difference in value when the vehicle passes first and when the pedestrian passes first. Golakiyaa et al. measured PVI at uncontrolled mid-block crosswalks using the SSM of time difference to collision (TDTC) in an attempt to classify levels of aggressive behavior exhibited by vehicles and pedestrians.

Trajectory-based PVI analyses have also been performed using LiDAR-based trajectories. Lv et al. proposed an automated method for identifying pedestrian-vehicle conflict events using speed-distance profiles (SDP) to break up the conflicts into different risk levels. Wu et al. also used road user trajectories extracted from LiDAR sensors to calculate a variety of SSM such as post encroachment time (PET), the proportion of the stopping distance (PSD), and crash potential index (CPI). These SSMs have also been applied to vehicle-to-vehicle interactions. Xie et al. utilized vision-based trajectories to identify rear-end conflicts at two intersections with 70-hours of total video recordings. Jiang et al. also studied vehicle-to-vehicle conflicts from vision-based trajectories to measure SSM such as PET, TTC, and DRAC for rear-end, lane changes, and fixed object conflicts on highways. Other interaction analyses can be done between vehicles and bicyclists, E-Bikes, and even wild animals.

Much of the literature on traffic trajectory applications is interactions between road users and measuring SSM. However, there is no method to automatically extract roundabout capacities and yield rates for pedestrians at uncontrolled crossings.

Methodologies

The methodologies for each application are outlined. First the data collection details are outlined. Then, the roadside LiDAR preprocessing is detailed to generate trajectory data. Finally, the methodologies for the two applications are outlined.

Data Collection

The data collection and extraction for the roundabout are outlined. The LiDAR data collection setup, as shown in Figure 1, consists of batteries and for powering a computer and the LiDAR sensor. The LiDAR sensor used is a 32-channel Velodyne LiDAR sensor operating at 10 hertz with 360-degree horizontal rotation and 10-degree scanning (+/-5 degrees) in the vertical direction. The data is stored in 30-minute .pcap files on an external hard drive. The raw LiDAR data can be seen through the Veloview software as shown in Figure 1.

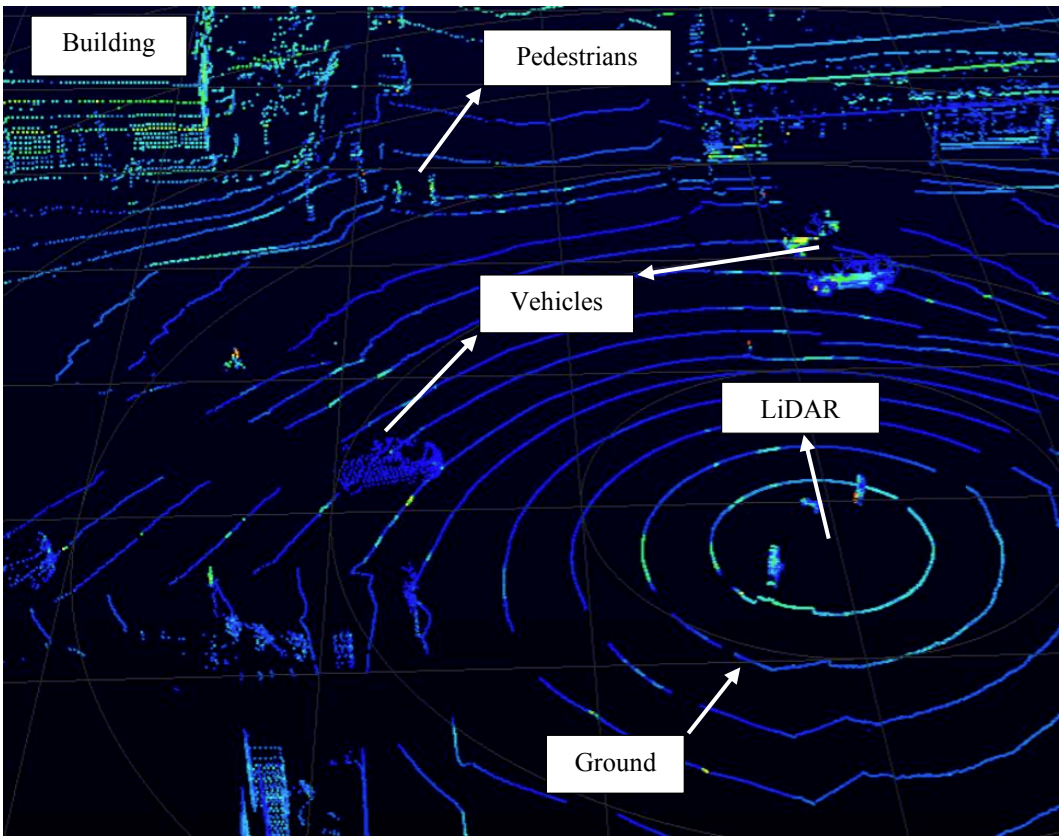

Figure 1 Raw LiDAR Data

Data Pre-Processing of Roadside LiDAR Data

The algorithm for data preprocessing of roadside LiDAR is outlined. Raw LiDAR data, as seen in Figure 1, needs to be pre-processed to extract trajectory information of all road users such as passenger vehicles, heavy vehicles, bicycles, pedestrians, and even wild horses. The methods outlined have been developed by a group of researchers from the same team. As such, a brief overview of the methodologies will be outlined. The stages for data pre-processing include background filtering, object clustering, object classification, real-time tracking of movement, and data mapping.

Background Filtering

Raw LiDAR data, as seen in Figure 1, includes the cloud points of everything from trees, buildings, the ground, and other static objects. As such it is important to filter out the background to increase the accuracy of object detection and classification and reduce the computational cost. The method is outlined by Zhao *et al*. Background filtering is performed first by aggregating multiple LiDAR data frames and dividing the point into small and continuous 3D cubes. The laser points contained in a 3D cube are identified as background cloud points if the number of laser points is greater than an automatically learned threshold. The background 3D cubes are used to identify the background laser points and the background laser points are excluded. The threshold laser point value depends on the distance the 3D cube is from the LiDAR sensor.

Object Clustering and Referencing

The purpose of clustering objects is to categorize road users based on similarities of laser points. These similarities can be the centroid, density, connectivity, and distribution of a cluster. The method employed for clustering objects is the density based spatial clustering application with noise (DBSCAN), which divides the dataset into core points, border points, and noise points within a predefined searching radius (Zhao *et al.* 2019). If the number of data points within the searching radius is greater than a predefined minimum number of points, the data points will be clustered into an object. However, the searching radius and minimum points parameters must be adjusted based on the road user type (vehicle vs. pedestrian), distance from the LiDAR sensor (closer cluster will have higher resolution), and the angle of the LiDAR

laser beam. An adaptive DBSCAN clustering algorithm has been documented in a previous study (Zhao *et al.* 2019).

Once the background has been filtered, the reference points of each road user are defined to track the clusters and extract trajectory information. For pedestrians, Zhao *et al.* used the mean center of each cluster as the reference point. For vehicles, the reference point is defined as the closest corner of the cluster to the LiDAR sensor as it provides the most accurate results. For instance, a vehicle traveling away from the sensor may use the back corner closest to it, while a vehicle traveling towards the sensor may use the front corner closest to it. Again, further details on this algorithm have been documented in a previous study (Zhao *et al.*, 2019).

Object Classification

There are several road users such as vehicles, pedestrians, and bicycles that utilize the roadway simultaneously. Therefore, it is critical to classify the previously clustered objects into the correct road user type. The total number of cloud points, 2D distance, and direction of the clustered point distribution are extracted from the object clustering process to classify the clustered objects. Using these three parameters, a backpropagation artificial neural network (BP-ANN) was developed to train for the classification of the clusters.

Object Tracking

With clustered object classified, the object tracking is performed to extract trajectory and speed information of the road users. The process of tracking is to identify the same object over continuous data frames (Zhao *et al.*, 2019). Two factors are considered for object tracking: the distance from one object in the previous frame to all objects in the current frame and the time difference between the two frames. The object in the current frame that is the closest to the object in the previous frame is the match of the two objects. The distance threshold is based on the speed limit. If the current object cannot be matched to a previous object, a new object ID is assigned to that object. Each road user has their own unique object ID.

Data Mapping

Once vehicle trajectories have been obtained, the next step is to map the data so the data is georeferenced and can be uploaded into ArcGIS for further analysis. The coordinate system for raw LiDAR data is a cartesian coordinate system with the LiDAR sensor as the origin. Tian *et al.* proposed a data mapping method for roadside LiDAR to convert the LiDAR coordinate system to the WGS-84 coordinate system. The method requires at least for reference points of LiDAR cartesian points and corresponding geographic coordinates to be collected by Trimble R2. Then, a transformation matrix is derived and used to convert the LiDAR data. This is an essential step in extracting the desired headway and speed information.

The final result for processing the LiDAR cloud points in the georeferenced trajectories of all road users as shown in Figure 2.

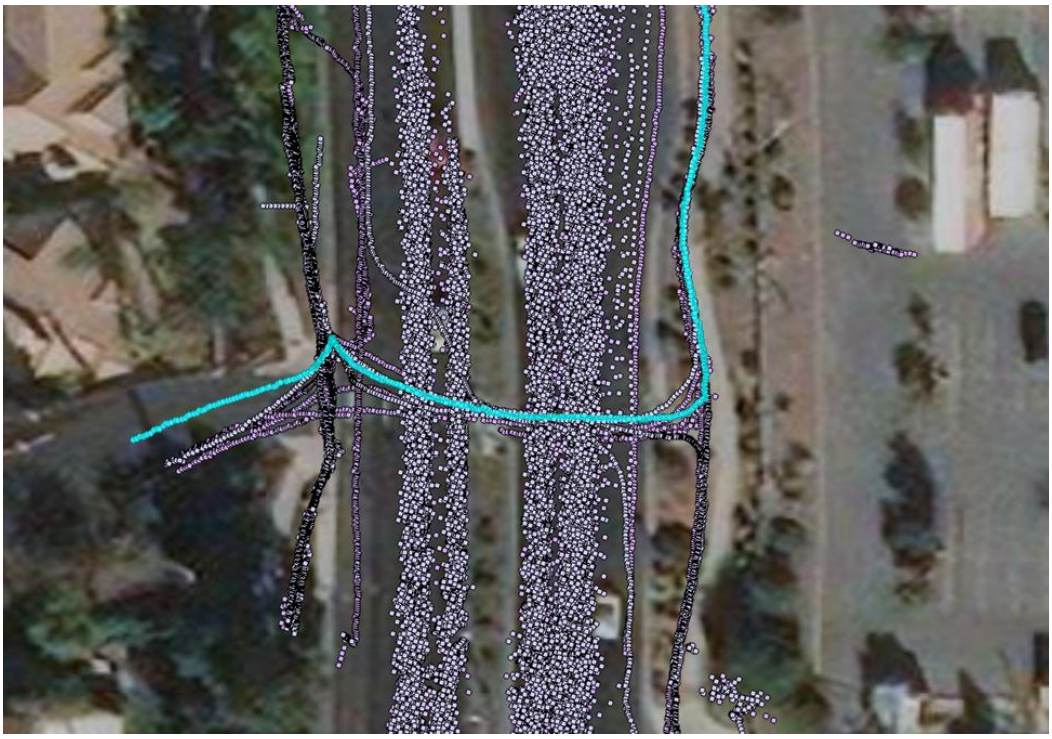

Figure 2 Georeferenced Trajectories of All Road Users

Roundabout Capacity Methodology

The methodology for extracting headway information from LiDAR trajectory data is outlined. This includes the methodology for extracting headway information. Then, the method for extracting the critical headway will be detailed. Finally, the method for calibrating the HCM capacity equation is outlined.

Roadside LiDAR Trajectory Headway Extraction

With the georeferenced trajectories of all road users obtained in the data preprocessing stage, the volume, speed, and trajectories can be extracted for specified detection zones for further analysis. First, the geolocated trajectory data is converted to GIS feature classes every 30 minutes. Then in ArcGIS, the detection zones are drawn for the entry lanes and conflicting circulatory lanes using the draw command and converting the drawings into feature classes; a schematic is shown in Figure 3. Next, an ArcGIS plugin of python scripts created by the authors is run to determine the volume, direction, size, and speed of each road user for each detection zone. From the output obtained by the python script, the desired input for headway extraction are outlined in Figure 3 and detailed as follows:

- Entry Vehicle Stop (E_{stop}): Timestamp for which the entry vehicle comes to a stop.
- Entry Vehicle Enters (E_{enter}): Timestamp for which the entry vehicle accepts the headway.
- Entry Average Speed (V_{avg}): Average speed of entry vehicle trajectory points in the detection zone.
- Circle Vehicle Enters Conflict Zone ($C_{conflict}$): Timestamp for which the circulating vehicle arrives at the conflict zone.

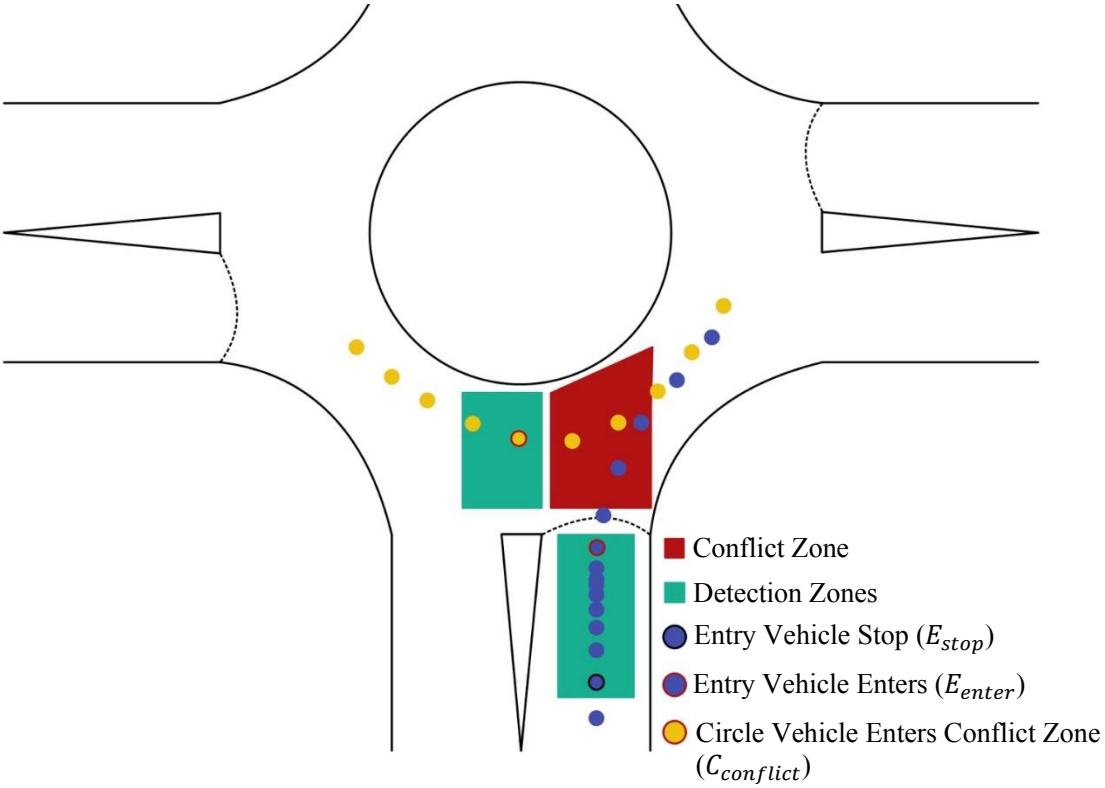

Figure 3 Vehicle Trajectories and ArcGIS Detection Zones

The data inputs outlined in Figure 3, are used to determine the following:

- Rejected lag: the time difference between an entry vehicle arriving at the yield line and a circulating vehicle arriving at the conflict zone for which the entry vehicles rejects.
- Accepted lag: the time difference between an entry vehicle arriving at the yield line and a circulating vehicle arriving at the conflict zone for which the entry vehicles accepts (does enter).
- Rejected Headway: the time difference between two following vehicles measured from the front bumper of the leading vehicle to the front bumper of the following vehicle for which a corresponding entry vehicle rejects.
- Accepted Headway: the time difference between two following vehicles measured from the front bumper of the leading vehicle to the front bumper of the following vehicle for which a corresponding entry vehicle accepts.
- Follow-up Headway: The time headway between queued entry vehicles utilizing the same headway in the conflicting circulatory flow.

For a rejected lag, the time difference between when an entry vehicle comes to a stop and the next circulatory vehicle enters the conflict zone is recored as the rejected lag if the entry vehicle does not enter the roundabout before the cirulatory vehicle enter the conflict zone. While this value is not used in this study, it may be used for further analysis in subsequent studies. Furthermore, it is essential to differentiate between rejected lags and rejected headways because the rejected headways are major stream headways that are observed by the minor stream decision vehicle whereas rejected lags are not.

For a rejected headway, when an entry vehicle remains in the detection zones while two or more vehicles in the circulatory lane pass the conflict zone, the corresponding circulatory headways are extracted and set a rejected headways. Alternatively, when the maximum frame index for the entry vehicle is in between two circulatory maximum frame indices, the entry vehicle entered the circulatory stream and the corresponding circulatory headway is recorded as an accepted headway.

The method for determining the lags and headways are illustrated in the flowchart shown in Figure 4.

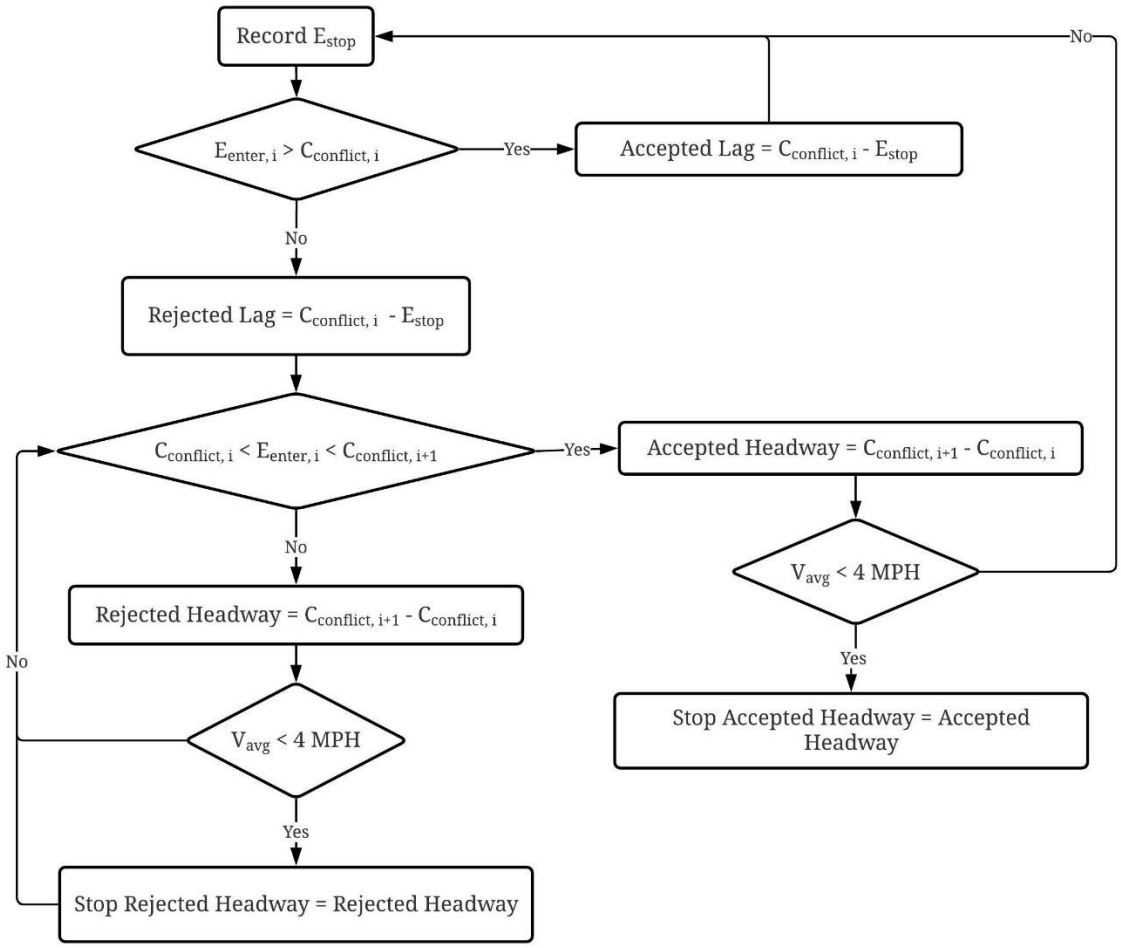

Figure 4 Flow Chart for Rejected and Accepted Headway Extraction

The follow-up headway is determined by measuring the headway of queued entry vehicles that enters the same circulating headway when the leading vehicle comes to a stop. Once the maximum frame index for the entering vehicle is recorded, the headway of the following queued vehicles is recorded. The maximum threshold defined is 5 seconds to ensure that only vehicles in the queue are recorded. The measurement is stopped once a new circulatory vehicle approaches the conflict zone or the entry headway exceeds 5-seconds.

Critical Headway and Follow-up Headway

Once the rejected and accepted headways are extracted, the critical headway is determined. The method that is used in this study is Raff's Method, in which the critical headway is determined graphically by finding the point of intersection between the following cumulative distribution functions:

$$1 - F(t_r) \text{ and } F(t_a) \quad (1)$$

Where;

$t_r = rejected\ headway$

$t_a = accepted\ headway$

$F = cumulative\ distribution\ Function$

HCM 2016 Capacity Equation Calibration

The method for calibrating the HCM 2016 capacity equations is outlined. Equations (2) – (4) outline the HCM calibration equations based on the inputs of critical headway, follow-up headway, and conflicting flow.

$$C = Ae^{(-Bv_c)} \quad (2)$$

$$A = \frac{3600}{t_f} \quad (3)$$

$$B = \frac{t_c - (\frac{t_f}{2})}{3{,}600} \quad (4)$$

Where;

$C = lane\ capacity, passenger\ cars\ (pc)/hr$

$v_c = conflicting\ flow, pc/hr$

$t_c = critical\ headway, seconds$

$t_f = follow-up\ Headway, seconds$

Pedestrian-Vehicle Yield Rate Extraction Methodologies

Two methodologies are proposed to extract yield rates between pedestrians and vehicles at uncontrolled crosswalks, the threshold and statistical methods.

Roadside LiDAR Trajectory Yield Input Data

With the georeferenced trajectory of all road users obtained in the data preprocessing stage, the desired yield parameters, such as vehicle speed and time to enter crosswalk, can be extracted for each trajectory in each specified detection zones. First, the geolocated trajectory data is converted to GIS feature classes every 30 minutes. Then in ArcGIS, the detection zones are drawn for the trajectory conflict points of interest, a schematic is shown in Figure 5. Next, an ArcGIS plugin of python scripts created by the authors is run to extract each pedestrian crossing events and each important yield parameters corresponding to the PVI. These parameters include time stamp for which the vehicle and pedestrian enters the crosswalk and corresponnding vehicle speeds.

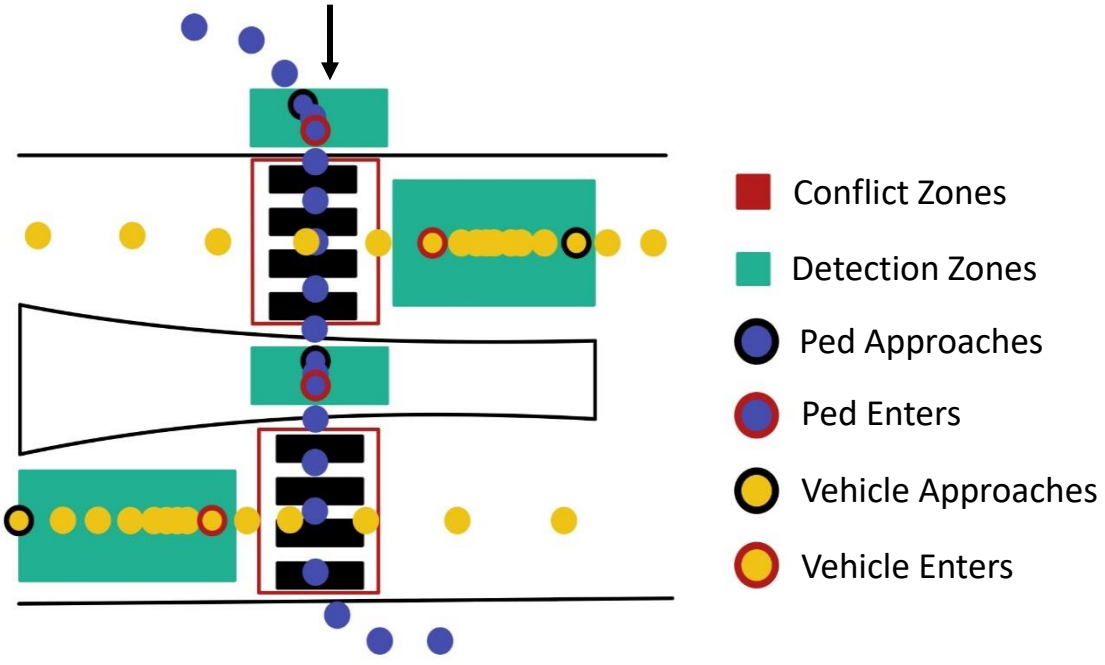

Figure 5 Vehicle and Pedestrian Trajectories and Detection Zones

Once the PVIs at the uncontrolled crosswalk are extracted through the Python Script, it is important to extract the yield information to know whether the vehicles yielded for pedestrians. Originally, the method was to measure the last trajectory point to leave the specifeied detection zone, which is the time stamp just before the vehicle or pedestrian enters the crosswalk. If the vehicle entered the croswalk before the pedestrian, then that was marked as a no yield case. If the pedestrian entered the crosswalk before the vehicle, then that was marked as a yield case. This timestamp between vehicles and pedestrians entering a crosswalk is also measured in the time difference to conflict (TDTC), which is the timestamp difference between the vehicle entering the crosswalk and the pedestrian entering the crosswalk. A positive value are yield cases while negative values are no yield cases.

However, there are several other considerations to be made to increase accuracy. First, only those crossing intances for which vehicles and pedestrians interact should be used. Next, the vehicle speed must be considered, which is important for ensuring vehicle actually yielded to pedestrians. Lastly, this method does not consider the stopping sight distance (SSD) for which a driver needs to preceive, react, and brake for a pedestrian crossing. Therefore, the data needs to be filtered to only include interactions between vehicles and pedestrians, and to only include vehicles that are physically able to yield. Once this is performed, every real vehicle-pedestrian yield interaction is collected with the following yield paramters:

1. Time difference to conflict (TDTC)
2. Vehicle speed

Threshold-Based Method for Extracting Vehicle-Pedestrian Yield Data

The first proposed methodology is to extrtact the yeild cases using theshold values. The first threshold value is the vehicle-pedestrian interaction threshold, which is defined by the crossing time for pedestrian through the crosswalk. If the TDTC is less than the pedestrian crossing time, this is considered an intereaction. Otherwise, the data is filtered out as a non-interaction case.The next threshold value is the vehicle speed threshold, which will mark whether the vehicle actually yielded. This is perhaps not as intuitive to gather because it varies based on the site. Also, it is not clear whether it is important to only consider full stops, or also floating vehicles. In this study, both are considered, which means a higher vehicle speed threshold value is used. The vehicle speed threshold value can be gleaned by looking at the raw LiDAR data, or by looking at the PVIs through a speed vs. TDTC plot. When there is sufficient data, the speed vs. TDTC plot shows clusters of data that could help identify possible speed thresholds. The final threshold has to do with SSD. In other words, it is important to exclude cases for which vehicles are unable to yeild for pedestrians. This is performed by calculating the SSD and converting it to stopping sight time. Then, this value is compared to the time difference between the “vehicle enters” and “ped approaches”, as shown in Figure 5. If the time difference is less than the stopping sight time, then the vehicle was able to yield, otherwise, the vehicle could not yield. Figure **6** is a flow chart illustrating the thershold-based method for extracting vehicle-pedestrian yield data.

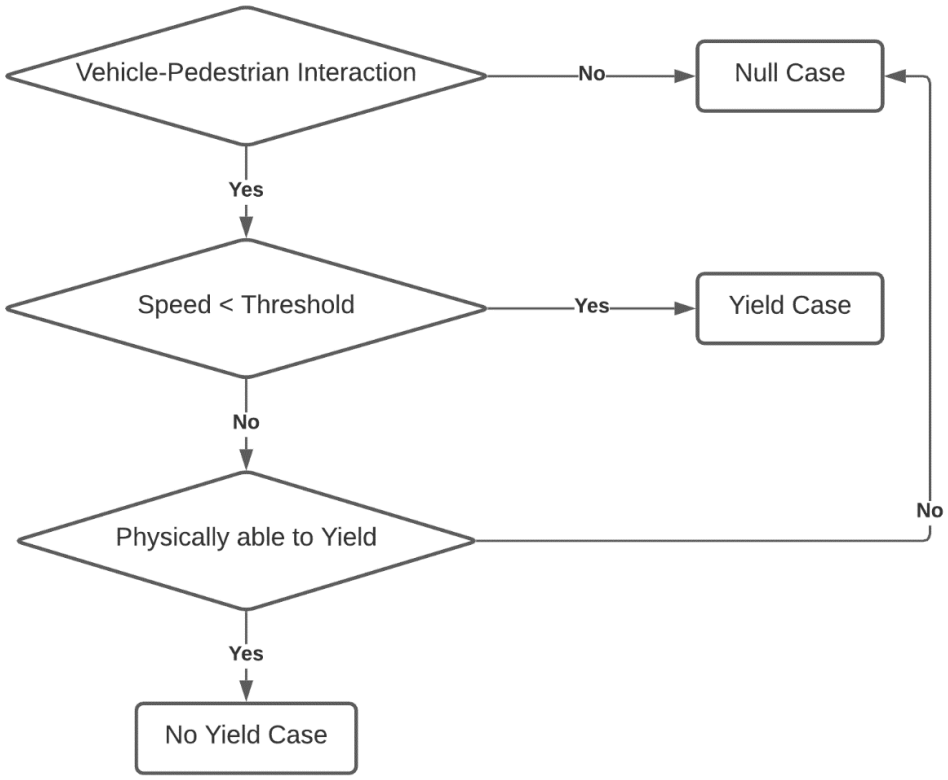

Figure 6 Threshold-Based Method for Extracting Vehicle-Pedestrian Yield Data

Statistical Method for Extracting Vehicle-Pedestrian Yield Data

The statistical method used for the yield extraction is discussed. This method seeks to fill gaps in understanding the variables that go into determining yield cases. Since such variables are continuous and PVI behaviors vary, it is perhaps more insightful to look into probabilities of yield cases to better understand these behaviors. First, the PVI data is filtered to only include true interactions and consider the SSD. With the data filtered, a statistical model is derived to extract vehicle-pedestrian yield data. The statistical method used in this paper is a logistic regression because the response variable is binary – yield versus no yield. The main covariates that are tested include the vehicle's speed and the TDTC. The general form of a logistic regression is written as such:

Linear model: $$y = b_0 + b_1 x \quad (1)$$

Logistic model: $$p = \frac{1}{1-e^{-(b_0+b_1 x)}} \overset{yields}{\Longleftrightarrow} \log\left(\frac{p}{1-p}\right) = b_0 + b_1 x \quad (2)$$

Where $y =$ Response, $b_0 =$ y-intercept, $b_1 =$ Slope, and $p =$ Probability of response

The first step is to generate real yield and no yield cases from the filtered PVI data. This is performed by going through each data point (interaction) and verifying whether it is a yield or no yield case by looking at the raw cloud point data. Once a sizeable sample has been manually compiled, the new dataset can be used to calibrate the model. Six models were tested in this paper, consisting of a combination of covariates vehicle speed, TDTC, and the binary of who entered the crosswalk first. For the best models, the logistic regression "S" curve is generated to see the continuous probability of yield or no yield

Case Studies

The case studies for the two applications is outlined. First, the roundabout capacity study is detailed, followed by the pedestrian-vehicle yield rate study. Both studies outline the site, apply the proposed methodologies, and share the results.

Roundabout Capacity

The case study for the roundabout capacity study is outlined. The study was conducted in Reno, Nevada, United States. The study roundabout is located in the South Reno residential area at the intersection of State Route (SR) 341 and Veterans Pkwy. Figure **7** on the left shows the roundabout and indicates the LiDAR sensor location, and Figure **7** on the right illustrates the georeferenced LiDAR trajectory results. For this study, only the south leg is considered. The south leg consists of two entry lanes that are yield controlled with the left – or inner – lane being a designated left-turn lane and the right – or outer – lane being a designated left-through-right lane. There is one corresponding conflicting – or circulatory – lane that is a designated through-left lane. Each entry lane will be considered separately for this study, with critical headway, follow-up headway, and capacity equations being determined for both. Vehicle trajectory data was collected at this roundabout using a LiDAR sensor. LiDAR data collection took place on Sunday, June 7th, 2020 from 9:00 AM – 9:00 PM with a 7-minute gap taking place from 3:00 PM – 3:07 PM. The traffic at this intersection is homogeneous and there were only 11 pedestrians for the full day on the south leg crosswalk. Therefore, heavy vehicle traffic and pedestrian factors are not considered.

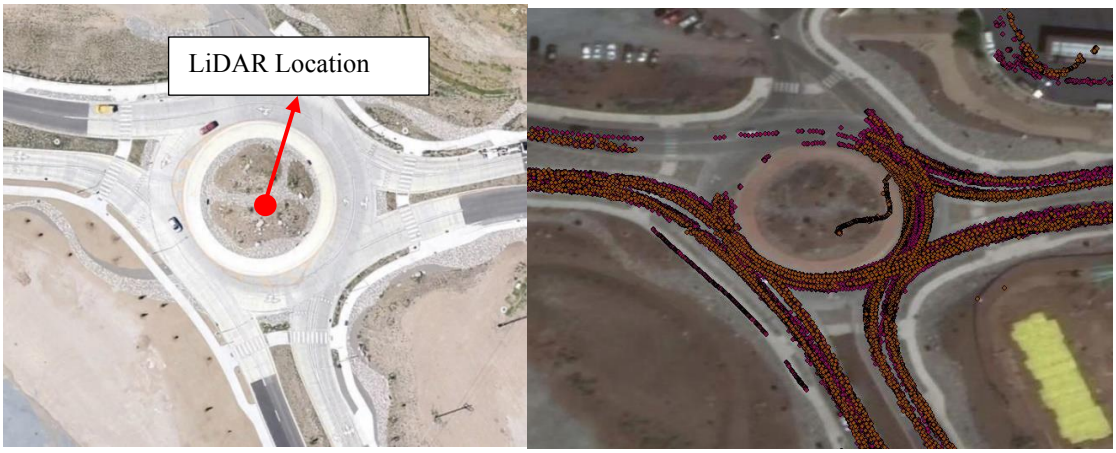

Figure 7 (left) Study Roundabout and LiDAR Locations and (right) Georeferenced LiDAR trajectory Results

Results and Analysis

The results and analysis of the data extraction are outlined. The rejected, accepted, and follow-up headways were recorded for the full 12-hour period of data collection. Table **1** shows the total number of rejected, accepted, and follow-up headways for the inner lane and outer lane. With higher traffic volumes determined for the outer entry lane, it is expected to see a greater number of headways for the outer lane.

Table 1 Total Number of Rejected, Accepted, and Follow-up Headways

Headway Type	Number of Headways Extracted	
	Inner	Outer
Rejected Headways	270	320
Accepted Headways	144	190
Follow-up Headways	79	204

Gap Acceptance Parameters

The results for the gap acceptance parameters for each entry lane are outlined. The first gap acceptance parameter is the critical headway. There have been many proposed methods for determining this value. The method that this study is using is Raff's Method because of its ease of computation for this case study. Figure 8 and Figure 9 illustrate Raff's Method plots for the inner lane and outer lane, respectively. The follow-up headway is determined by taking the average of all the follow-up headways. The critical headways and follow-up headways for both the inner and outer lanes are tabulated in Table 2. The acceptable range of accepted headways used was 3 – 10 seconds as 10 seconds adequately captures real headways that are observed by the driver. Longer headways were not considered because they could not be reasonably observed by the driver. The lower thresholds ensure that no errors show up. It was observed that accepted headways lower than 3 seconds is due to detection zone issues of vehicles not following the usual travel lane path.

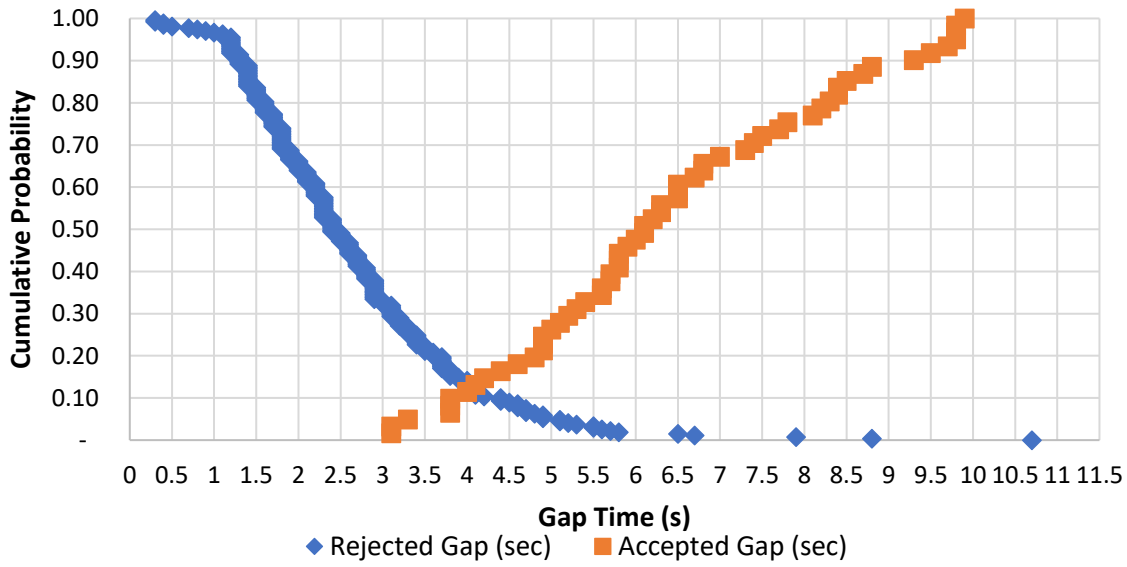

Figure 8 Raff's Method Cumulative Distribution Plot for the Inner Lane

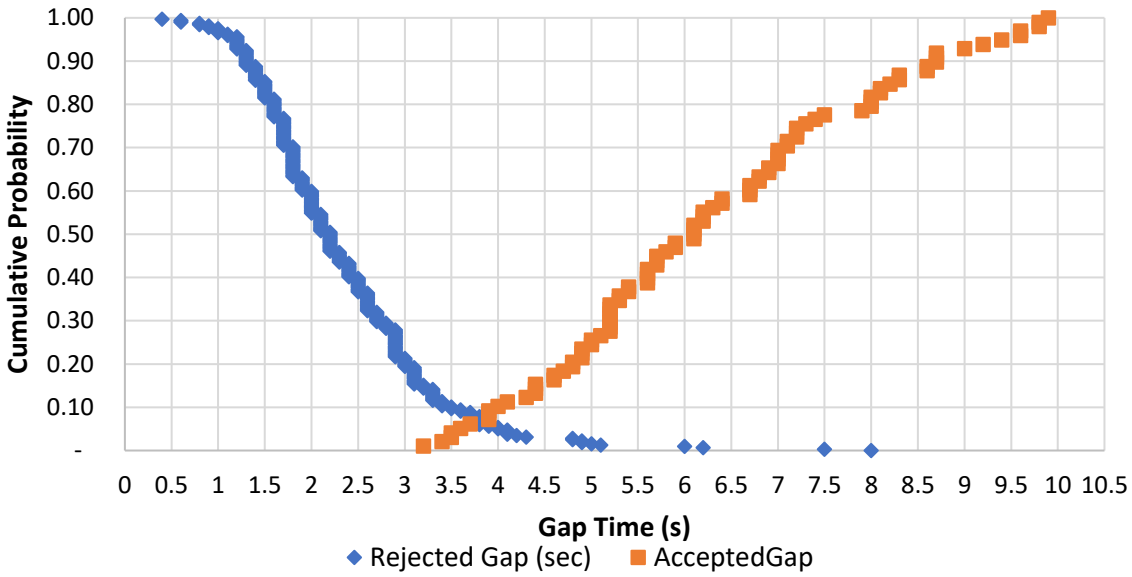

Figure 9 Raff's Method Cumulative Distribution Plot for the Outer Lane

Table 2 Critical Headway and Follow-up Headway

Lane	Inner Lane (sec)	Outer Lane (sec)	Percent Difference
Critical Headway (sec)	4.2	3.9	7.4%
Follow-up Headways (sec)	2.6	2.5	3.9%

HCM Calibration

The HCM calibration is conducted for both entry lanes based on the gap parameter results and is compared to the HCM 2016 and Nevada calibrations. Equation 5 is the capacity equation for the HCM 2016, Equation 6 is the capacity equation derived for the State of Nevada, Equation 7 is the capacity equation for the study inner lane, and Equation 8 is the capacity equation for the study outer lane. Figure **10** graphically represent the difference between each capacity equation.

$$C = 1{,}420e^{(-0.91\times10^{-3})v_c} \quad (5)$$

$$C = 1{,}230e^{(-0.67\times10^{-3})v_c} \quad (6)$$

$$C = 1{,}385e^{(-0.81\times10^{-3})v_c} \quad (7)$$

$$C = 1{,}440e^{(-0.74\times10^{-3})v_c} \quad (8)$$

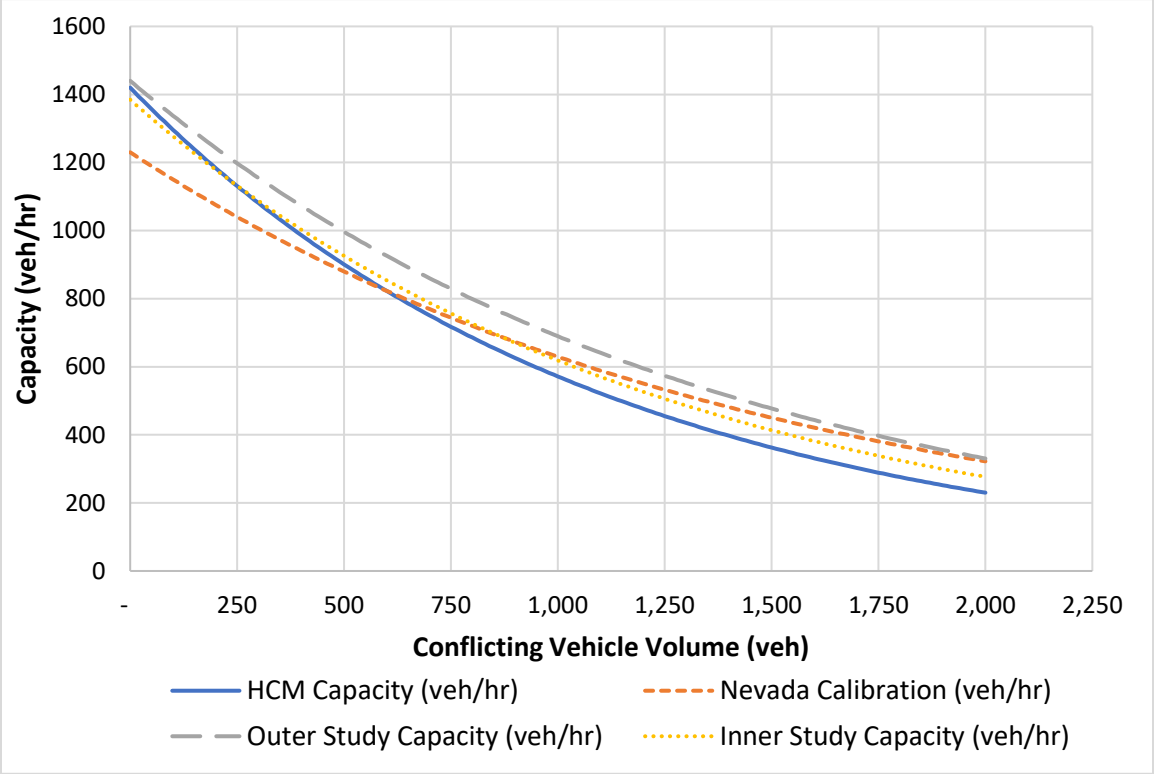

Figure 10 Capacity Equation Curves from the Study, HCM, and Nevada Calibrations

Pedestrian-Vehicle Yield Rates

The case study for his report will be outlined. The study was conducted in Henderson, Nevada, United States at an uncontrolled mid-block crosswalk at Green Valley Pkwy and Amargosa Trail. The crossing is equipped with a rectangular rapid flashing beacon (RRFB) activated by a push-button pressed by the pedestrians to alert drivers of their intent to cross. Figure **7** on shows the mid-block crosswalk and indicates the LiDAR sensor location. For this study, only the westbound pedestrian crossings and corresponding northbound vehicle movements are considered. There are two northbound lanes which are analyzed together. The all-road users cloud point data was collected at this crosswalk using a LiDAR sensor for the purposes of generating the trajectories of all road users. LiDAR data collection took place from 6/23/2019 8:00 AM to 6/29/2019 11:00 PM. The vehicle traffic at this intersection is mostly passenger vehicles and the crosswalk is used by pedestrians and bicyclists.

Figure 11 Study Mid-Block Crosswalk and LiDAR Location

Results and Analysis

The results and analysis of the yield data extraction are outlined. The PVI and corresponding vehicle speeds and timestamps are extracted for the full data collection period. There was a total of 866 PVIs recorded, which is also the same as the total number of pedestrians/bicycles crossing westbound.

Threshold-Based Method for Extracting Vehicle-Pedestrian Yield Data

The results for the threshold-based method are outlined. For this method, three threshold values need to be determined as follows:

- PVIs
- Vehicle speed
- SSD

To help understand these thresholds, we will take a look at the speed vs TDTC plot shown in Figure 12. To help understand how to read the speed-TDTC plot, it is good to break the data into quadrants as such:

I. Non-interaction cases where the vehicles speeds are uninterrupted by the pedestrian → high TDTC, high vehicle speed

II. Non-interaction cases where the vehicles speeds are interrupted, hence there are fewer data points → high TDTC, low vehicle speed

III. Interactions where the vehicles speeds are interrupted, hence making up a cluster of yield cases → low TDTC, low vehicle speed

IV. Interaction cases where the vehicle enters the crosswalk before the pedestrian and does not slow down, hance making a cluster of no yield cases → high TDTC, high vehicle speed

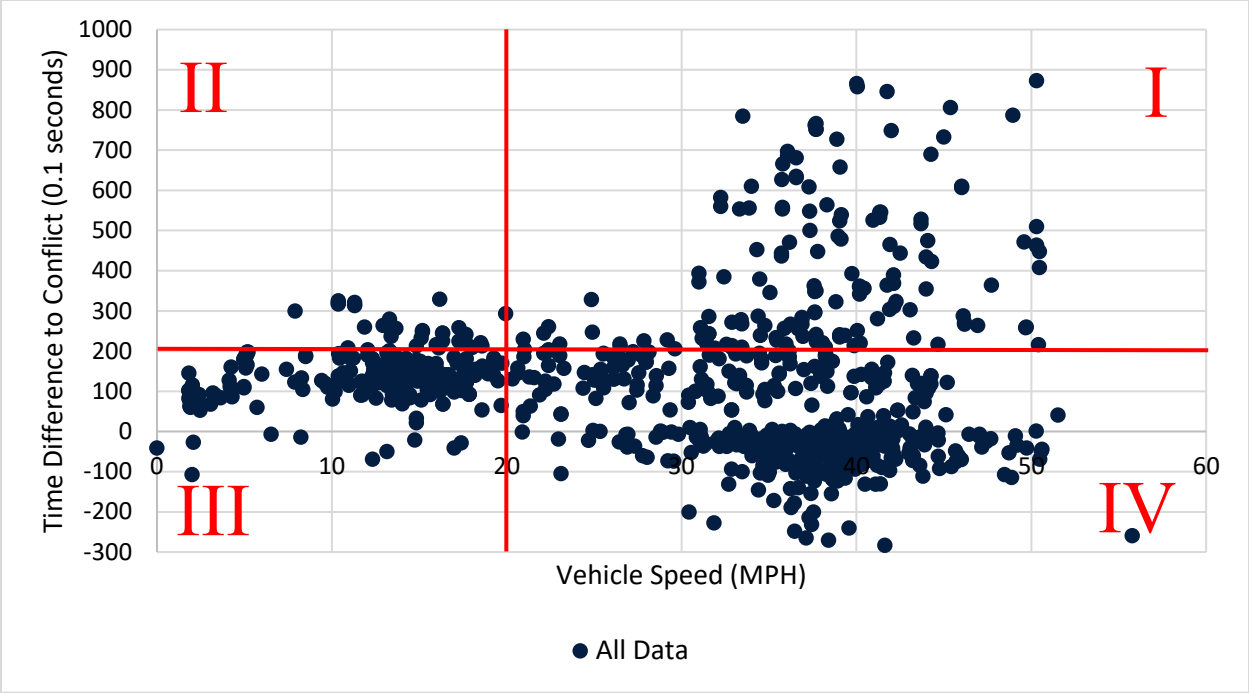

Figure 12 Speed vs TDTC plot

For the PVI threshold, the crossing time is used, which is based on the crosswalk length and a pedestrian speed of 3 feet per second. The value for this site is 20 seconds, so any TDTC that is greater than 20 seconds is filtered out as a non-interaction case A total of 309 points are filtered out non-interaction cases, which makes up 36% of the original data. Next, the vehicle speed threshold is determined. Given the speed limit of Green Valley Pkwy is 35 miles per hour (MPH), the threshold must be lower than the speed limit, but still large enough to capture the cluster shown in Figure 12. Based on manual observations, a vehicle speed threshold of 20 MPH was chosen. Finally, the SSD is considered, which is based on each individual vehicle speed and compared to the "vehicle enters" and "ped approaches" difference. SSD filtering will take points away from quadrant IV, which is the no yield quadrant. A total of 133 points were removed from the stopping sight distance filtering, leaving a total of 412 points. Figure 13 shows the filtered data and designates the yeild points and no yeild points. As shown in Table **3**, there was 190 yield cases and 222 no yield cases for a yield compliance of 46%.

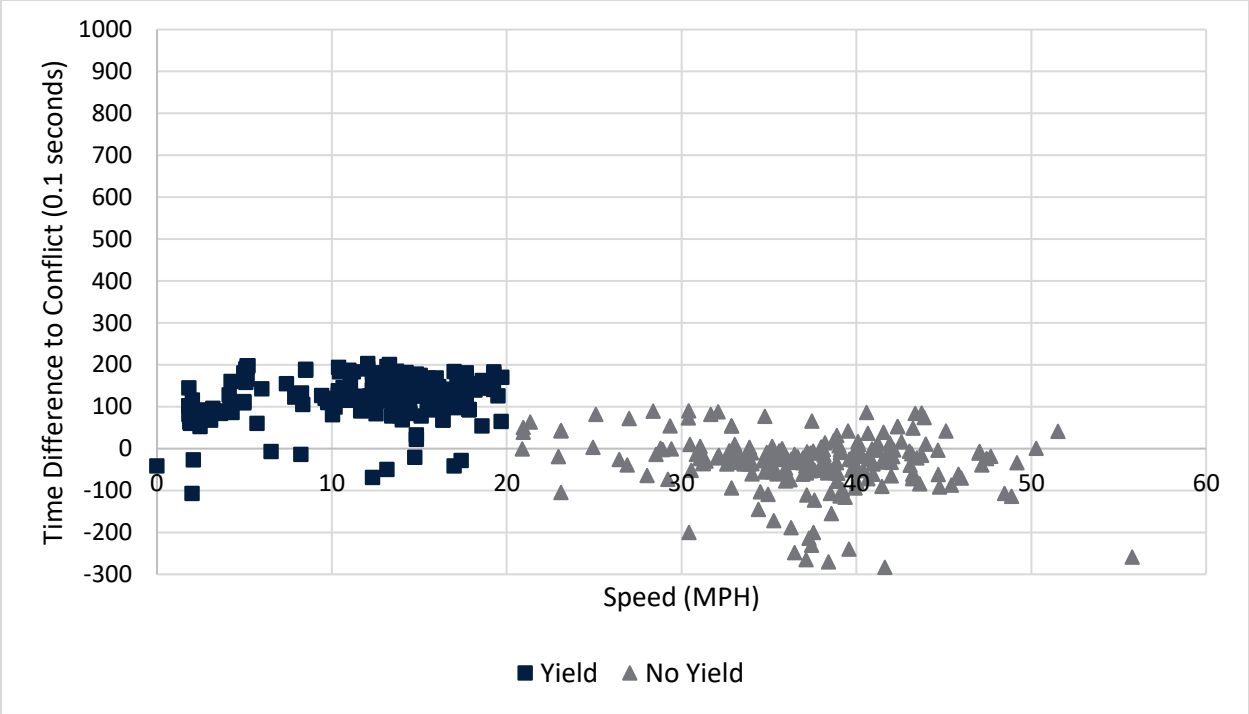

Figure 13 Filtered Speed vs TDTC plot

Table 3 Yield counts and yield compliance

Yield Cases	No Yield Cases	Yield Compliance
190	222	46%

Statistical Method for Extracting Vehicle-Pedestrian Yield Data

The process for determining the best logistic regression for the statistical method is discussed. The first step is to filter the non-interactions and based on the SSD, which leaves us with the same 412 data points. Then, a sample of real yield and no yield data is manually extracted from the raw LiDAR cloud points. 35 yields and 43 no yield for a total of 78 data points were manually extracted for the purposes of testing logistic regression models. The following models with corresponding variables are tested:

1. Vehicle speed
2. TDTC
3. Vehicle speed and TDTC
4. TDTC and pedestrian enters crosswalk first binary applied to the slope and intercept
5. Vehicle Speed and pedestrian enters crosswalk first binary applied to the slope and intercept
6. Vehicle Speed and TDTC with pedestrian enters crosswalk first binary applied to the slope and intercept

Each of the logistic regression model equations are outlined in Table **4** along with the Akaike information criterion (AIC). AIC is a mathematical method for evaluating how well a model fits the data. The lower AIC is, the better the model fits to the data. AIC typically is used to compare models. In the case of the models and corresponding AIC outlined in Table **4**, it appears that vehicle speed is the best parameter for determining yield cases since each model that has vehicle speed as one of its' parameters has a lower AIC. Figure **14** and Figure **15** illustrate the logistic regression curve for Model 5 and 6, respectively. From the curves, it can be gleaned that there is very low uncertainty in the probability of vehicles yielding to pedestrians. Not only does this validate the yield data, but it also emphasizes the importance of vehicle speed in determining yield rates.

Table 4 Logistic Regression Model Results

ID	Logistic Regression Models	AIC
1	$\log\left(\frac{P}{1-P}\right) = 8.40275 - 0.36194V$	25.443
2	$\log\left(\frac{P}{1-P}\right) = -1.049140 + 0.027741T$	56.053
3	$\log\left(\frac{P}{1-P}\right) = 6.838362 + 0.007509T - 0.305876V$	26.58
4	$\log\left(\frac{P}{1-P}\right) = -2.605406 - 0.006273T - 8.209077d + 0.182603Td$	42.567
5	$\log\left(\frac{P}{1-P}\right) = 4.210 - 20.96V + 45.84d - 20.62Vd$	20.536
6	$\log\left(\frac{P}{1-P}\right) = 4.27011 - 0.25015V - 0.01886T - 6.85780d + 0.14556Td$	25.128

* Where $P = probability, V = vehicle\ speed, T = TDTC, d = ped\ enter\ first\ binary$

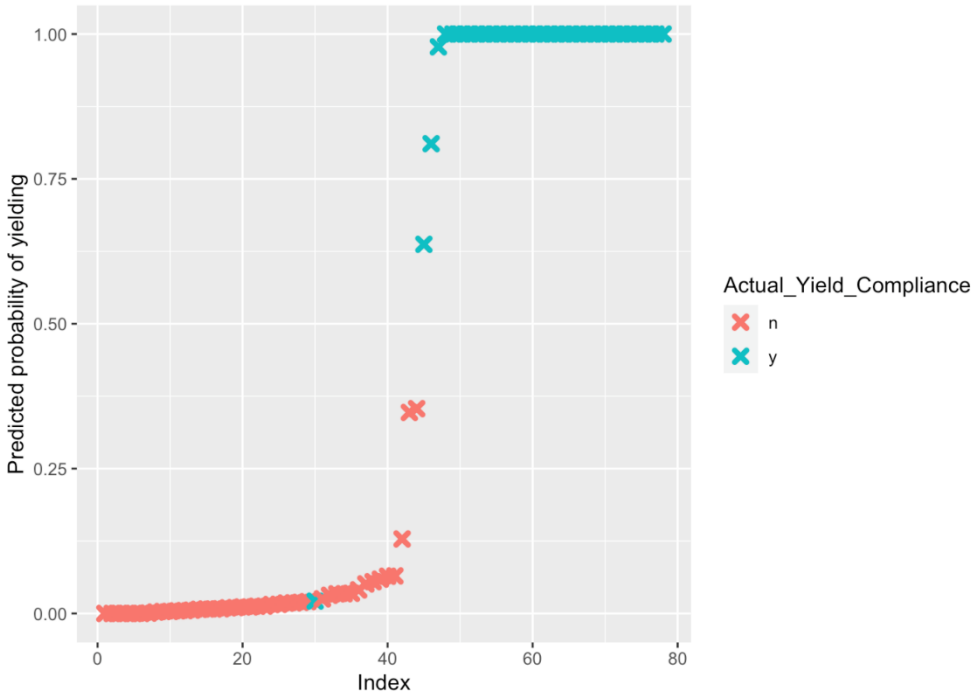

Figure 14 Logistic Regression Curve for Model 5

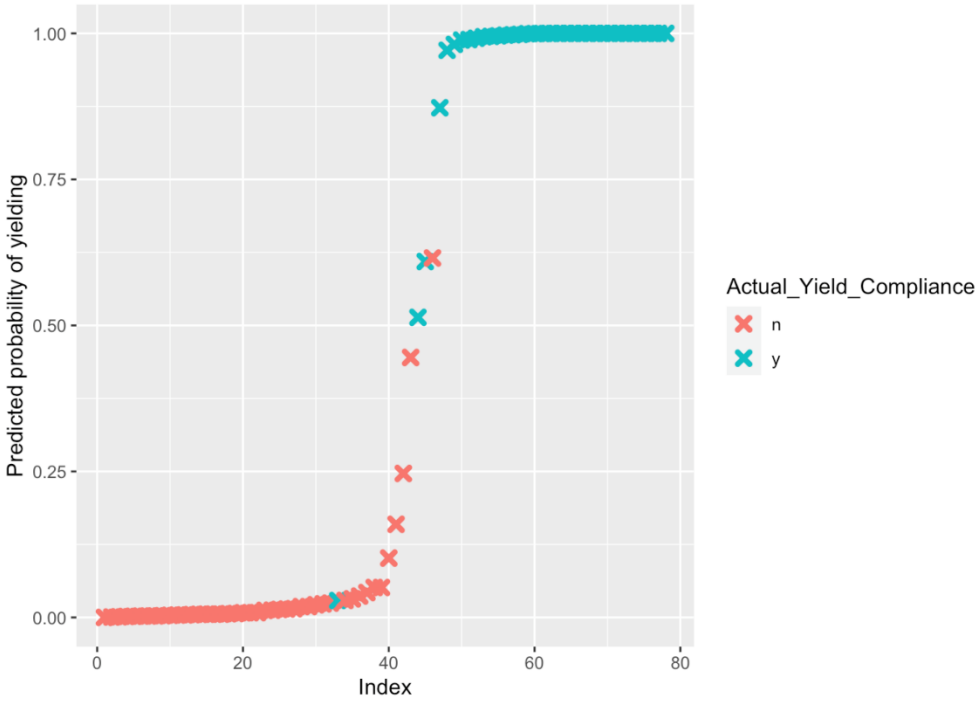

Figure 15 Logistic Regression Curve for Model 6

Conclusions

The concluding remarks and extended studies for both applications are detailed.

Roundabout Capacity

The purpose of the roundabout capacity application was to propose an automatic method to extract headway information from roadside LiDAR trajectory data. The purpose of this study was to propose an automatic method to extract headway information from roadside LiDAR trajectory data. A new method was proposed in this paper and tested in the field on a roundabout in Reno, NV to generate headway and capacity information. With the validation of the results with the HCM 2016 and Nevada capacity equations, the automatic method proposed in this paper proved to provide similar results to industry standard equations. Thus, operational information such as headway and capacity for roundabouts, used by industry traffic engineers across the country, can be provided at much faster rates by using the method proposed in this paper.

Extended studies that can be derived from this paper for roundabouts include analyzing the other legs of this roundabout, considering the high pedestrian volumes recorded at the east leg on Monday, June 8th, 2020, analyzing roundabout data with high heavy vehicle volume, analyzing data collected at small roundabout, and considering the exiting vehicle and priority reversal in the algorithm. The methodology proposed in this paper have also been applied to vehicle-pedestrian interactions at unsignalized crosswalks such as two-way stop-controlled intersections, roundabouts, and mid-block crosswalks via yield rate extracting. The proposed method could also provide unique analyses at merging situations at freeway on-ramps.

Pedestrian-Vehicle Yield Rates

This study aimed at developing an automated method for extracting yield rates from PVIs at uncontrolled crosswalks using real world roadside LiDAR trajectory data. In the literature, much of the yield rate data was performed through manual methods. Trajectory data is used for PVI studies, but the focus is more on SSMs such as PET and TTC. Two methods were presented for extracting yields from trajectory data. The

threshold method is a great way to easily extract yield rates at a variety of sites. The statistical method is perhaps more robust, but requires that the model is recalibrated to the variability of new sites and situations. While these methods performed well, there are a number of limitations that will be considered in future studies. In the literature review, the presence of pedestrian groups played a significant role in yield rate. Future methods will seek to aggregate data corresponding to pedestrians' groups. Furthermore, there a number of bicyclists that cross of the case study location which will be taken into account for future models. Determining whether the crossing interaction occurred during platoons is another aspect that can easily be considered. Pedestrian assertiveness measures through waiting time and pedestrian gap acceptance will also considered to analyze the pedestrian behavior.

In the future, similar analyses will be performed for other uncontrolled crosswalks such as roundabout and one-to-two-way stop-controlled intersections. Furthermore, before-after studies of yield rates will be done before and after the installation of an RRFB, as well as the before and after automatic RRFBs. Similar studies can be performed at signalized intersections at right turn movements and conflicting pedestrian crossing events. Such a study could be used to evaluate the effectiveness of leading pedestrian intervals (LPI). Finally, further expansion to other SSMs such as PET and TTC can be studied to identify risk levels at intersections or roadways and identify near-crash events.

References

1. TRB. *Highway Capacity Manual Edition 6, Chapter 22, Roundabouts.* Transportation Research Board, National Research Council, Washington DC, USA, 2016.
2. Ahiamadi, S. K., Z. Tian, and A. R Gibby. *Nevada Roundabout Implementation Guidelines.* Publication Report No. 079-10-803. Nevada Department of Transportation, 2012
3. World Health Organization. Global Status Report on Road Safety 2018; World Health Organization: Geneva, Switzerland, 2018.
4. Amado, H., Ferreira, S., Tavares, J. P., Ribeiro, P., and Freitas, E. Pedestrian-Vehicle Interaction at Unsignalized Crosswalks: A Systematic Review. *Sustainability.* 2020.
5. Kizawi, A,. and Borsos, A. A literature review on the conflict analysis of vehicle-pedestrian interactions. *Acta Technica Jaurinensis.* Vol. 14, No. 4, 2021, pp. 599-611.
6. Fu, t., Miranda-Moreno, L., and Saunier, N. A novel framework to evaluate pedestrian safety at non-signalized locations. *Accident Analysis and Prevention.* No. 111, Elsevier. 2018, pp. 23-33.
7. Zhao, J., Xu, H., Liu, H., Wu, J., and Zheng, Y. Detection and tracking of pedestrians and vehicles using roadside LiDAR Sensors. *Transportation Research Part C: Emerging Technologies.* Vol. 100. 2019. pp. 68-87.
8. TRB. *Roundabouts: An Informational Guide Second Edition.* NCHRP Report 672. Transportation Research Board, National Research Council, Washington, DC, USA, 2010.
9. Rodergerdts, L. *Applying Roundabouts in the United States.* NCHRP Report 3-65. Transportation Research Board, National Research Council, Washington, DC, USA, 2004.
10. TRB. *Highway Capacity Manual Edition 5, Chapter 21, Roundabouts.* Transportation Research Board, National Research Council, Washington, DC, USA, 2010.
11. Rodergerdts, L., Blogg, M., Wemple, E., Myers, E., Kyte, M., Dixon, M., List, G., Flannery, A., Troutbeck, R., Brilon, W., Wu, N., Persaud, B., Lyon, C., Harkey, D., and Carter, D. *Roundabouts in the United States.* NCHRP Report 572. Transportation Research Board, National Research Council, Washington, DC, USA, 2007.
12. United States Department of Transportation (USDOT). *Accelerating Roundabouts in the United States: Volume II of VII - Assessment of Roundabout Capacity Models for the Highway Capacity Manual*. Publication FHWA-SA-15-070. United States Department of Transportation Washington D.C. 2015.
13. Xu, F. and Z. Tian. Driver Behavior and Gap-Acceptance Characteristics at Roundabouts in California. In *Transportation Research Record: Journal of the Transportation Research Board,* No. 2071, Transportation Research Board of National Academies, Washington, D.C., 2008, pp. 117-124.
14. Azhari, S. F., Puan, O. C., Hassan, S. A., Mashros, N., Warid, M. N., and Lopa, R. S. *IOP Conference Series: Material Science and Engineering*. Vol. 527. 2019.
15. Guo, R. J. Estimating Critical Gap of Roundabout by Different Methods. *6th Advanced Forum on Transportation of China (AFTC 2010)*. 2010.
16. Hamad, H. A. *Investigation of Gap Acceptance at Roundabouts in Qatar.* Masters thesis. Qatar University, Doha, Qatar, 2017.
17. Shaaban, K., and H. Hamad. Critical Gap Comparison Between One-, Two-, and Three-Lane Roundabouts in Qatar. *Sustainability,* Vol. 12, No. 10, 2020
18. Sun, d., Benekohal, R. F., and Ukkusuri, S. V. Modeling of motorist-pedestrian interaction at uncontrolled mid-block crosswalks. In *Transportation Research Record: Journal of the Transportation Research Board,* Transportation Research Board of National Academies, Washington, D.C., 2003.
19. Ottomanelli, M., Lannucci, G., and Sassanelli, D. Simplified Model for Pedestrian-Vehicle Interactions at Road Crossings Based on Discrete Events System. In *Transportation Research Record: Journal of the Transportation Research Board,* No. 2316, Transportation Research Board of National Academies, Washington, D.C., 2012, pp. 58-68.
20. Feliciani, C., Gorrini, A., Crociani, Luci., and Vizzari, G. A simulation model for non-signalized pedestrian crosswalks based on evidence from on field observation. *Intell. Artif.* 2017, No. 11, pp. 117–138.
21. Chen, P., Wu, C., and Zhu, S. Interactions between vehicles and pedestrians at uncontrolled mid-block crosswalks. *Safety Science* No. 82, Elsevier. 2016, pp. 68-76.

22. Schroeder, B., Rouphail, N., Salamati, K., Hunter, E.; Phillips, B., Elefteriadou, L., Chase, T., Zheng, Y., Sisiopiku, V., Mamidipalli, S. Empirically-based performance assessment and simulation of pedestrian behavior at unsignalized crossings. Southeastern Transportation Research, Innovation, Development and Education Center (STRIDE). 2014.
23. Schroeder, B.J., and Rouphail, N.M. Event-based modeling of driver yielding behavior at unsignalized crosswalks. *J. Transp. Eng*. 2010, 137, 455–465.
24. Fricker, J. D. and Zhang, Y. Modeling Pedestrian and Motorist Interaction at Semi-Controlled Crosswalks: The Effects of a Change from One-Way to Two-Way Street Operation. In *Transportation Research Record: Journal of the Transportation Research Board,* No. 2673, Transportation Research Board of National Academies, Washington, D.C., 2019, pp. 433-446.
25. Lu, L., Ren, G., Wang, W., Chan, C., and Wang, J. A cellular automata simulation model for pedestrian and vehicle interaction behavior at unsignalized mid-block crosswalks. *Accident Analysis and Prevention*. No. 95, Elsevier. 2016, pp. 425-437.
26. Schneider, R., Sanatizadeh, A., Razaur, M., Shaon, R., He, Z., and Qin, Z. Exploratiary Analysis of Driver Yielding at Low-Speed, Uncontroled Crosswalks in Milwaukee, Wisconsin. In *Transportation Research Record: Journal of the Transportation Research Board,* No. 2672, Transportation Research Board of National Academies, Washington, D.C., 2018, pp. 21-32.
27. Fitzpatrick, K. and Park, E. Nighttime effectiveness of pedestrian hybrid beacons, rectangular rapid flashing beacons, and LED-embedded crossing sign. *Journal of Safety Research.* No 79, Elsevier. 2021, pp. 273-286
28. Coughenour, C., Abelar, J., Pharr, J., Chien, L., and Singh, A. Estimated car cost as a predictor for driver yielding behavior for pedestrians. *Journal of Transport and Health.* No. 16, Elsevier. 2020.
29. Salamati, K., Schroeder, B. J., Geruschat, D. R., and Rouphail, N. M. Event-Based Modeling of Driver Yielding to Pedestrains at Two-Lane Roundabout Approaches. In *Transportation Research Record: Journal of the Transportation Research Board,* No. 2389, Transportation Research Board of National Academies, Washington, D.C., 2013, pp. 1-11.
30. Bell, F., and Nobili, F. Driver-pedestrian interaction under legal and illegal pedestrian crossings. *Transportation Research Procedia.* No. 45, Elsevier. 2020, pp. 451-458.
31. Fu, t., Hu, W., Miranda-Moreno, L., and Saunier, N. Investigating secondary pedestrian-vehicle interactions at nonsignalized intersections using vision-based trajectory data. *Transportation Research Part C*. No. 105, Elsevier. 2019, pp. 222-240.
32. Muppa, K., Kumar, C., and Tallam, T. Vehicle Pedestrian Interaction Analysis at Unsignalized Intersections using Trajectory Data. *2022 IOP Conf. Ser.: Earth Environ. Sci. 962* 012057. 2022.
33. Golakiya, H., Chauhan, R., and Dhamaniya, A. Mapping Pedestrian-Vehicle Behavior at Urban Undesignated Mid-Block Crossings under Mixed Traffic Environment – A Trajectory- Based Approach. *Transportation Research* No. 48, Elsevier. 2020, pp. 1263-1277.
34. Lv, B., Sun, R., Zhang, H., Xu, H., and Yue, R. Automatic Vehicle-Pedestrain Conflict Identification With Trajectories of Road Users Extracted From Roadside LiDAR Sensors Using a Rule-Based Method. *IEEE Access.* vol. 7, 2019, pp. 161594-161606.
35. Wu, J., Xu, H., Zhang, Y., and Sun, R. An Improved vehicle-pedestrian near-crash identification method with a roadside LiDAR Sensor. *Journal of Safety.* No. 73, 2020, pp. 211-224.
36. Xie, K., Ozbay, K., Yang, H., and Li, C. Mining Automatically extracted vehicle trajectory data for proactive safety analytics. *Transportation Research Part C.* No. 106, Elsevier. 2019, No. 61-72.
37. Jiang, R., Zhu, S., Chang, H., Wu, J., Ding, N., Liu, B., and Qiu, J. Determining an Improved Conflict Indicator for Highway Safety Estimation Based on Vehicle Trajectory Data. *Sustainability*. No. 13, 2020.
38. Tian, Y., Xu, H., and Wu, J. A Data Mapping Method for Roadside LiDAR Sensors. *2019 IEEE Intelligent Transportation Systems Conference (ITSC).* Auckland, New Zealand. 2019.